Effects of tune modulation on particles trapped in one-dimensional resonance islands

Y. Wang,[1] M. Ball,[1] B. Brabson,[1] J. Budnick,[1] D. D. Caussyn,[1] A. W. Chao,[2] J. Collins,[1] V. Derenchuk,[1] S. Dutt,[2] G. East,[1] M. Ellison,[1] D. Friesel,[1] B. Hamilton,[1] H. Huang,[1] W.P. Jones,[1] S.Y. Lee,[1] D. Li,[1] J.Y. Liu,[1] M.G. Minty,[1] K.Y. Ng,[3] X. Pei,[1] A. Riabko,[1] T. Sloan,[1] M. Syphers,[2] Y.T. Yan,[2] and P.L. Zhang[2]

[1]*Indiana University Cyclotron Facility, Indiana University, Bloomington, Indiana 47405*

[2]*The Superconducting Super Collider Laboratory, 2550 Beckleymeade Avenue, Dallas, Texas 75237-3946*

[3]*Fermilab, P.O. Box 500, Batavia, Illinois 60510*

(Received 18 October 1993)

The response of particles trapped in one-dimensional resonance islands to betatron tune modulation resembles, yet is not equivalent to, that of a parametric resonant system. Experimental data obtained at Indiana University Cyclotron Facility for the fourth-order resonance islands have confirmed this characteristic feature. The beam, driven by betatron tune modulation, was observed to travel from near the center of resonance islands toward the separatrix. The experimental data are characterized by the onset of a large response at a critical modulation amplitude and frequency, which are compared with theoretical models. Possible future experiments are suggested.

PACS number(s): 41.85.−p, 05.45.+b, 29.20.Dh

I. INTRODUCTION

Enhanced particle diffusion in a dynamical system due to a time dependent driving force has long been recognized [1]. This problem is particularly important to high energy colliders and high brightness storage rings, where the time dependent components usually play a key role in determining the dynamical aperture and particle stability. The time dependent driving components in high energy storage rings can be divided into dipole field modulation and quadrupole field modulation. The dipole field modulation can arise from ground vibration or current ripple in dipoles. Similarly, the quadrupole field modulation can come from current ripple in quadrupoles, synchrotron motion with nonzero chromaticities, and/or the feed down of sextupoles resulting from ground vibrations etc. In the past we have studied the effects of longitudinal beam dynamics due to dipole field modulation and/or rf acceleration field modulation [2–5]. This paper studies specifically transverse beam dynamics due to the betatron tune modulation, which was generated by modulating the current supplied to a quadrupole. We study, in particular, effects of tune modulation on particles trapped in resonance islands. Such a tune modulation would generate regions of stochastic layers in the phase space of otherwise invariant tori. These stochastic layers may cause an enhanced diffusion rate.

Many theoretical and numerical particle tracking studies [6,7] have investigated the effects of betatron tune modulation. It was recognized that the effect of tune modulation on particles trapped in resonance islands is equivalent to a system of a physical pendulum with phase modulation [1]. Reference [6] obtained the condition of chaos from the particular solution of the linearized pendulum equation. However, the linear superposition is known to break down near the region of the island resonance frequency [4], where the nonlinearity plays an important role in the dynamics. Alternatively, Ref. [7] defined the width of the stochastic layer as the relative deviation of the Hamiltonian value from separatrix orbit. The change of relative energy deviation, calculated along the separatrix orbit for a half period of the time dependent perturbation, is a function of the phase angle of the particle relative to the time dependent driving potential. On the other hand, the phase angle depends, in turn, on the relative energy change. The stability of the coupled equations is then used to obtain the critical width of the stochastic layer. In particular, the width of the stochastic layer is found to be maximum when the modulation frequency is equal to about 1.35 times the island frequency at a constant modulation amplitude. Numerical simulations in Ref. [7] seem to confirm that tori of the resonance Hamiltonian are strongly affected around that modulation frequency at a constant modulation amplitude. Experimental confirmation of these different approaches is therefore needed. These experiments also offer a unique opportunity to check various theoretical models in the study of long term stability for particle beams in circular accelerators.

In the past, there were several experiments on effects of betatron tune modulation [8,9]. However, these tune modulation experiments were not able to track single particle motion in the Hamiltonian system. In the CERN experiments [8], lifetime of the beam was measured as a function of the tune modulation amplitude at a combination of modulation frequencies of 9 Hz, 40 Hz, and 180 Hz. These modulation frequencies were chosen to sample regions of interest. On the other hand, the range of modulation frequencies was chosen near the resonance island frequency for the Fermilab experiment [9]. However, because of the small island size, only the rate of decoherence as a function of the modulation frequency for the beam captured in the island was measured. Tracking single particle motion inside an island could not be performed. To understand single particle dynamics, it is important to be able to follow the trajectory of a single particle in the dynamical system.

To measure a single particle motion, small beam emittance is needed. In this respect, the Indiana University Cyclotron Facility (IUCF) cooler ring provides an ideal environment for nonlinear beam dynamics experiments. The 95% emittance, or phase space area, of the proton beam is electron cooled to about 0.3 π mm mrad in less than 3 s. The resulting relative momentum spread full width at half maximum, FWHM, of the beam is about 0.0001. Such a high quality beam bunch can closely simulate single particle motion shown evidently in our earlier experimental results [2–5].

This paper reports results of experiments performed at the IUCF cooler ring on the effect of tune modulation for particles trapped in resonance islands. We organize this paper as follows. Section II discusses Hamilton's equation of motion in the presence of tune modulation for particles trapped in resonance islands of 1 degree of freedom [one dimension (1D)]. Section III discusses the experimental procedure and presents experimental data. Conclusions are given in Sec. IV.

II. THE EQUATION OF MOTION IN THE PRESENCE OF TUNE MODULATION

The Hamiltonian in the action-angle variables in a region dominated by a single resonance ($m\nu = \ell$) is given by

$$H = \nu J + \frac{1}{2}\alpha J^2 + gJ^{\frac{n}{2}}\cos(m\phi - \ell\theta + \chi) + \cdots, \quad (1)$$

where J and ϕ are the conjugate action-angle variables for the betatron oscillations, θ is the orbital angle serving for the time coordinate, ν is the betatron tune (either horizontal or vertical), α is the nonlinear betatron detuning parameter arising from higher-order multipoles, g and χ are the resonance strength and phase at the 1D nonlinear resonance $m\nu = \ell$ with integral m, ℓ, and $n \geq m$. For particles with small actions, the term with $n = m$ dominates the dynamics [10]. Hereafter, we consider the Hamiltonian with $n = m$ only.

Using the generating function,

$$F_2 = \left(\phi - \frac{\ell}{m}\theta + \frac{\chi}{m}\right) I, \quad (2)$$

we transform the coordinate system into the resonance rotating frame where the new action-angle coordinates are given by $I = J$ and $\psi = \phi - \frac{\ell}{m}\theta + \frac{\chi}{m}$. The new Hamiltonian becomes

$$\tilde{H} = \delta I + \frac{1}{2}\alpha I^2 + gI^{\frac{m}{2}}\cos m\psi. \quad (3)$$

Here $\delta = \nu - \frac{\ell}{m}$ is the proximity of the betatron tune to the resonance line. The transformed Hamiltonian is time independent and is a constant of motion. A torus corresponds to the Hamiltonian flow at a constant "energy," i.e., $\tilde{H}(I, \psi) = E$.

This simple single resonance dominated Hamiltonian has been verified experimentally [11,12] for the third- and the fourth-order resonances by comparing the measured Poincaré maps with tori of the Hamiltonian. Hamilton's equations of motion are given by

$$\dot{I} = mgI^{\frac{m}{2}}\sin m\psi, \quad (4)$$

$$\dot{\psi} = \delta + \alpha I + \frac{m}{2}gI^{\frac{m}{2}-1}\cos m\psi, \quad (5)$$

where the dot represents the derivative taken with respect to the orbital angle θ. The fixed points (I_f, ψ_f) of the Hamiltonian are given by

$$\sin m\psi_f = 0 \quad \text{and} \quad \delta + \alpha I_f \pm \frac{m}{2}gI_f^{\frac{m}{2}-1} = 0. \quad (6)$$

Thus the fixed points are local extrema of the Hamiltonian along a line of constant ψ, i.e.,

$$\frac{\partial}{\partial I}E\bigg|_{\sin m\psi = 0} = 0.$$

The unstable fixed point (UFP) corresponds to a saddle point on the energy surface, while the stable fixed point (SFP) corresponds to a local extremum.

In particle accelerators, the betatron tunes may be time dependent due to quadrupole current supply ripple. With a small tune modulation, the parameters α and g do not vary appreciably. The equation for the phase oscillations becomes

$$\ddot{\psi}_m + G\sin\psi_m = m\ddot{\delta}, \quad (7)$$

where $\psi_m = m\psi$ signifies the *island* phase angle and G is the spring constant for the phase oscillation given by

$$G = \frac{m^3}{2}EgI^{\frac{m}{2}-2} + \frac{m^2}{4}(m-4)\alpha gI^{\frac{m}{2}}. \quad (8)$$

Thus the phase oscillations generally resemble the physical pendulum equation. However, when $m \neq 4$, the spring constant G depends on the action, which is time dependent. In fact G is not necessarily positive definite in the entire region of a torus. In the linearized approximation, i.e., $\sin\psi_m \approx \psi_m$, the island tune is given by "ν_{island}" $= \sqrt{G}$. We sometimes loosely use $\sqrt{G}$ as the "island tune." The actual island tune $\tilde{\nu}_{\text{island}}$, of a given torus can be obtained from solving Hamilton's equations of motion, i.e.,

$$\tilde{\nu}_{\text{island}} = 2\pi m\left[\oint \frac{dI}{(g^2I^m - [E - \delta I - \frac{1}{2}\alpha I^2]^2)^{1/2}}\right]^{-1}. \quad (9)$$

Since the spring constant is not necessarily a constant, the phase oscillation may not be uniform within a torus of the Hamiltonian flow. The phase oscillation of Eq. (7) with the addition of tune modulation resembles, but is *not* equivalent to, the pendulum equation with phase modulation. The difference is that the spring constant depends also on the amplitude. Thus the effect of tune modulation on the island motion will depend critically on resonance parameters. This effect was not considered in earlier theoretical analyses [6,7]. Nevertheless, the island

tune for small amplitude oscillations of Eq. (9) becomes

$$\nu_{\text{island}} = \frac{m}{2}\,[2mE_{\text{SFP}}gI_{\text{SFP}}^{\frac{m}{2}-2} + (m-4)\alpha g I_{\text{SFP}}^{\frac{m}{2}}]^{1/2}. \quad (10)$$

An accidental cancellation occurs at the fourth order resonance with the result that the island tune is given by $\nu_{\text{island}} = \sqrt{32Eg}$, which is constant for a given torus. Since the energy E is an extremum at the SFP, the island tune will be largest at the SFP. In the following, we will discuss two low-order resonances.

A. The third-order resonance

At the third-order resonance with $m = 3$, fixed points of the Hamiltonian are given by

$$I_f^{1/2} = \frac{\mp\frac{3}{2}g \pm \sqrt{(\frac{3}{2}g)^2 - 4\alpha\delta}}{2\alpha}. \quad (11)$$

It is clear that the third-order resonance fixed points exist when the condition

$$g^2 \geq \frac{16}{9}\alpha\delta \quad (12)$$

is satisfied. We obtain therefore

$$I_{\text{SFP}}^{1/2} = \frac{\frac{3}{2}|g| + \sqrt{(\frac{3}{2}g)^2 - 4\alpha\delta}}{2|\alpha|}, \quad (13)$$

$$I_{\text{UFP}}^{1/2} = \frac{\left|\frac{3}{2}|g| - \sqrt{(\frac{3}{2}g)^2 - 4\alpha\delta}\right|}{2|\alpha|}.$$

Note here that if $\alpha\delta > 0$, then the SFP and UFP are located on the same betatron phase angle, i.e., $\psi_{\text{SFP}} = \psi_{\text{UFP}}$. On the other hand, if $\alpha\delta < 0$, then the betatron phase angles of the SFP and the UFP differ by 60°, i.e., $\psi_{\text{SFP}} = \psi_{\text{UFP}} \pm \frac{\pi}{3}$. The energy at the fixed point is given by $E_f = \frac{1}{3}\delta I_f - \frac{1}{6}\alpha I_f^2$, where I_f is either I_{SFP} or I_{UFP}, and the corresponding small amplitude island tune becomes $\nu_{\text{island}}^2 = \frac{9}{2}g\sqrt{I_{\text{SFP}}}(\delta - \alpha I_{\text{SFP}})$. An illustrative example is given in the Appendix.

B. The fourth-order resonance

The equation for phase oscillation at the fourth-order resonance with $m = 4$ has a particularly simple feature. Assuming $\alpha > 0$, the fixed points are given by

$$I_{\text{SFP}} = -\frac{\delta}{\alpha - 2|g|}, \quad I_{\text{UFP}} = -\frac{\delta}{\alpha + 2|g|}, \quad (14)$$

and the corresponding "energies" at these fixed points are

$$E_{\text{SFP}} = -\frac{\delta^2}{2(\alpha - 2|g|)}, \quad E_{\text{UFP}} = -\frac{\delta^2}{2(\alpha + 2|g|)}. \quad (15)$$

Note here that the fourth-order resonance island exists only when both the conditions $\alpha\delta \leq 0$ and $\alpha > 2|g|$ are satisfied. When the resonance strength $|g|$ is larger than $\frac{1}{2}|\alpha|$, the SFP of the fourth-order resonance island goes to infinity, while the UFP's are still given by Eq. (14). Similar results can be arrived at for $\alpha \leq 0$.

The small amplitude island tune becomes

$$\nu_{\text{island}} = 4|\delta|\sqrt{\frac{|g|}{\alpha - 2|g|}}. \quad (16)$$

Since the equation of motion for the betatron phase is given by

$$\ddot{\psi}_4 + 32Eg\sin\psi_4 = 0,$$

the island tune for a torus around the resonance island will depend on two factors: (1) the energy factor E, which is a constant for a given torus, and (2) the amplitude of the synchrotronlike motion. In other words, the phase oscillation of the fourth-order resonance is "equivalent" to that of synchrotron motion. When the betatron tune is modulated, the equation of motion for particles trapped in the island becomes a parametric resonance equation with phase modulation [Eq. (7)]. The response of a system having such an equation of motion exhibits bifurcation when the modulation frequency lies below the critical frequency. Such a system has recently been studied extensively for synchrotron motion [2–4].

The separatrix (the torus passing through the UFP) separates the island motion from tori inside and outside. The minimum and maximum actions of the separatrix are given by

$$I_{\text{sx1}} = I_{\text{SFP}}\left(1 + 2\sqrt{\frac{|g|}{\alpha + 2|g|}}\right), \quad (17)$$

$$I_{\text{sx2}} = I_{\text{SFP}}\left(1 - 2\sqrt{\frac{|g|}{\alpha + 2|g|}}\right).$$

It is interesting to note that the average of the maximum and minimum actions of the separatrix is equal to the action of the SFP. The island width is given by

$$\Delta I = I_{\text{sx1}} - I_{\text{sx2}} = 4I_{\text{SFP}}\sqrt{\frac{|g|}{\alpha + 2|g|}}. \quad (18)$$

III. EXPERIMENTAL PROCEDURE AND RESULTS

The IUCF cooler ring is hexagonal with a circumference of 86.8 m. The experiment started with a 90 MeV H_2^+ beam strip injected, stored, and cooled in a 10 s cycle resulting in a 45 MeV proton beam. The stored beam consisted of a single bunch, typically with 3×10^8 protons and a bunch length of about 5.4 m (or 60 ns) FWHM for

this experiment. The revolution period in the accelerator was 969 ns with bunching produced by operating a rf cavity with frequency $f_0 = 1.031\,68$ MHz at harmonic number $h = 1$.

Before making a measurement, the injected beam was electron cooled for about 3 s. The stability of the horizontal closed orbit was measured to be better than 0.05 mm FWHM. The beam was then kicked with various angular deflections θ_K, with a pulsed deflecting magnet having a time width of 600 ns FWHM, and rise and fall times of 100 ns. The kick occurred in conjunction with a triple coincidence among a signal from the data acquisition system, the rf system which was providing the beam bunching, and a 7 s delay from the beginning of the injection cycle. Details of our experimental setup have been previously published [11].

Once perturbed by the kicker, the beam executed coherent betatron motion and sampled existing field nonlinearities in the synchrotron. The Poincaré map in (x-p_x) phase space was obtained by measuring the horizontal position deviations from the closed orbit at two different positions [11]. The transverse electron cooling time was typically about 1 s or 10^6 revolutions, which had a very small effect within the time of a measurement (4096 revolutions [13]). Nevertheless it was turned off 20 ms before the beam was kicked in order to avoid damping of the betatron oscillations.

In our earlier experiments [11], we found that the SFP's for the third-order resonance were located outside the dynamical aperture of the cooler ring. On the other hand, the properties of the fourth-order resonance island were successfully explored [12], we chose to study the effect of tune modulation for the beam trapped in the fourth-order resonance island. The horizontal betatron tune was chosen close to the fourth-order resonance condition, $\nu_x \approx 3.75$. The linear coupling between the horizontal and vertical betatron motion was corrected by a pair of skew quadrupoles [11,12,14]. A horizontal kicker was pulsed to kick the bunch into the center of the resonance island. Almost 100% of the particles in the bunch were trapped inside the island. After the kick, the power supply for a quadrupole was modulated sinusoidally [15]. The droop of the modulation quadrupole gradient as a function of modulation frequency due to the skin effect of the vacuum chamber was measured and compensated for up to about 3 kHz [15]. With tune modulation, the betatron tune was given by

$$\nu = \nu_0 + q \sin \nu_m \theta, \tag{19}$$

where the modulation amplitude q varied from 0.000 25 to 0.001.

With the rf phase feedback loop turned on, the momentum-deviation amplitude of the bunched beam coherent synchrotron oscillation has been measured to be less than 1×10^{-5}. Combining with the measured horizontal chromaticity of about -8, the betatron tune modulation due to the coherent synchrotron oscillation of the bunch was about 8×10^{-5} at the synchrotron frequency of about 200 Hz. The FWHM incoherent momentum spread of the bunch was about $\left(\frac{\Delta p}{p_0}\right)_{\text{FWHM}} \approx 8.5 \times 10^{-5}$, thus the incoherent tune modulation due to the momentum spread of the beam was about 7×10^{-4} at the synchrotron frequency of 200 Hz. Since the synchrotron frequency

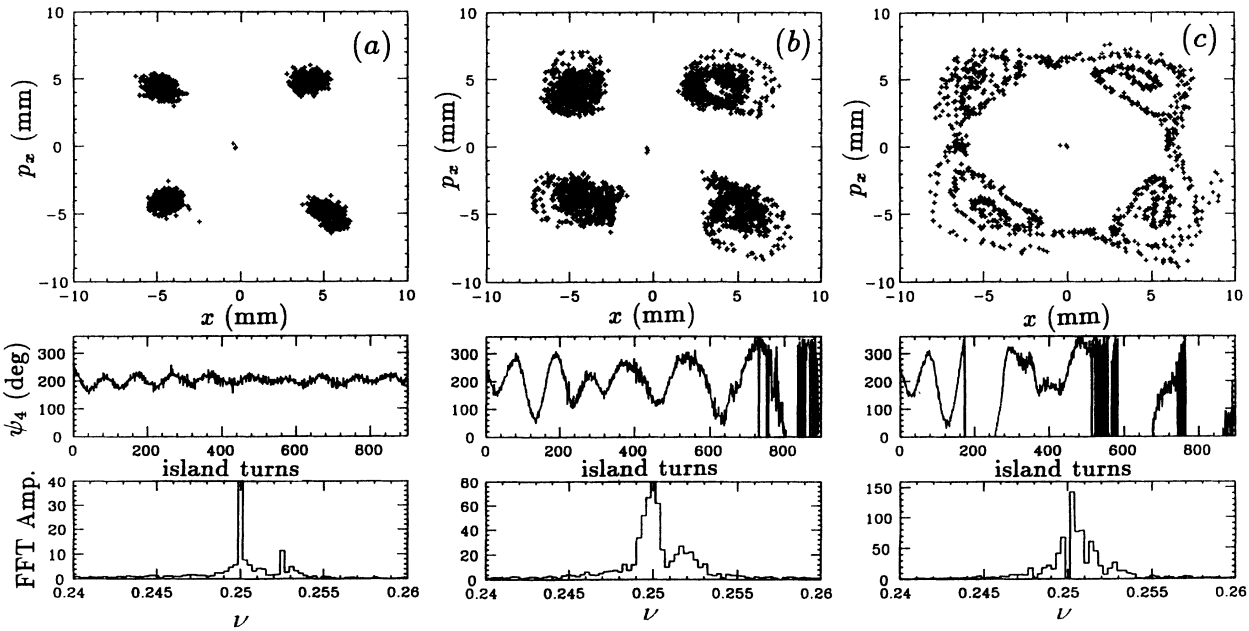

FIG. 1. The fourth-order resonance island motion without tune modulation is shown in the left column (a), where the top graph shows the Poincaré map for a beam bunch trapped in the fourth-order 1D resonance island, the middle graph shows the betatron phase oscillations of $\psi_4 = 4\psi$ of an island, and the bottom graph shows the FFT of the position coordinate. The effects of island motion due to tune modulation at the modulation frequencies of 1545 Hz and 2570 Hz at the modulation amplitude of $q = 0.000\,86$ are shown in (b) and (c) columns, respectively.

was chosen to be much smaller than the resonance island frequency, the effect of tune modulation due to the synchrotron oscillation and the finite chromaticity on particles trapped in the fourth-order resonance islands should be negligible.

A. Poincaré maps and the resonance Hamiltonian

Figure 1(a) in the left column shows (1) the Poincaré map in (x, p_x) phase space for 3584 orbital revolutions at the top, (2) the betatron phase ψ_4 of one of the islands as a function of the island turns (the number of orbital revolutions divided by the number of islands) in the middle, and (3) the fast Fourier transform (FFT) of the betatron oscillations at the bottom, for the beam bunch trapped in the fourth-order resonance islands *without* applying betatron tune modulation. The data points located at the origin of the Poincaré map in Fig. 1(a) correspond to beam bunch positions prior to the coherent betatron kick. From the bottom frame of Fig. 1(a), the island tune is observed as a sideband of the betatron tune to be $\nu_{\text{island}} = 0.002\,63 \pm 0.0003$ or the island frequency $f_{\text{island}} = 2720$ Hz. This means that our data acquisition system [13] was able to sample about nine island oscillations clearly visible from the middle part of Fig. 1(a). Because the synchrotron tune was much smaller than the island tune, the data indicated that the effect of the natural tune modulation due to a finite chromaticity and the synchrotron oscillation of the beam bunch was small.

Figure 1(b) shows similar data for the bunch motion with forced tune modulation at the modulation frequency, $f_m = 1545$ Hz and $q = 0.000\,86$, where 2000 orbital revolutions are plotted in the Poincaré map. Figure 1(c) shows data at $f_m = 2570$ Hz and $q = 0.000\,86$, where 1000 orbital revolutions are plotted in the Poincaré map.

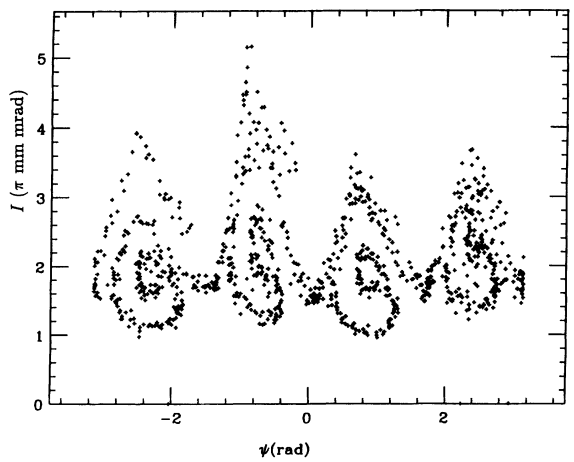

FIG. 2. The Poincaré map in action-angle variables for the bunch trapped in fourth-order resonance islands under the external betatron tune modulation at the modulation frequency of 2570 Hz for the same data as that shown in Fig. 1(c). Note here that the particle is driven out of the island onto the separatrix of the resonance Hamiltonian in about 640 orbital revolutions.

At a relatively large tune modulation amplitude of $q = 0.000\,86$, Figs. 1(b) and 1(c) show that the particle motion in the island was strongly perturbed. When the modulation frequency was 1545 Hz, the bunch was driven out of the island in about 700 island turns, or 2800 orbital revolutions. The phase oscillations of ψ_4, shown in the middle of Fig. 1(b), exhibit an interesting beating oscillation similar to that observed for synchrotron motion with rf phase modulation [3,4]. At the modulation frequency of 2570 Hz, the bunch was driven out of the island in about 160 island turns or 640 orbital revolutions and traveled along the separatrix of these islands.

Transforming the normalized phase space coordinates into the action-angle variables [11] for the modulation frequency at 2570 Hz, Fig. 2 shows that the beam bunch moves from a nearly center position in resonance islands to a trajectory along the separatrix. The maximum and minimum actions of the separatrix and the actions of the SFP and UFP are thus determined to be

$$I_{\text{sx1}} = 3.7 \pm 0.2\ \pi\,\text{mm mrad},$$

$$I_{\text{sx2}} = 1.1 \pm 0.2\ \pi\,\text{mm mrad},$$

$$I_{\text{SFP}} = 2.4 \pm 0.2\ \pi\,\text{mm mrad},$$

$$I_{\text{UFP}} = 1.5 \pm 0.2\ \pi\,\text{mm mrad}.$$

Using Eqs. (16) and (17), parameters for the resonance Hamiltonian can be obtained as

$$\begin{aligned} &\alpha = 1.0 \times 10^{-3}\ (\pi\,\text{mm mrad})^{-1}, \\ &g = -9.8 \times 10^{-5}\ (\pi\,\text{mm mrad})^{-1}, \quad \chi = 0.75\ \text{rad}, \\ &\delta = -1.9 \times 10^{-3}. \end{aligned} \tag{20}$$

These parameters are found to be consistent with the I_{UFP} of Eq. (14). An overall sign for the Hamiltonian is not determined from this method unless the nonlinear detuning parameter α is measured. The actual overall sign in the Hamiltonian is, however, not important with regards to the dynamics in the presence of tune modulation.

B. Beam response due to tune modulation

When the betatron tune is externally modulated, the equation of motion for the island phase is given by

$$\ddot{\psi}_4 + \nu_{\text{island}}^2 \sin\psi_4 = \nu_m^2 a \cos\nu_m\theta, \tag{21}$$

where $\psi_4 = 4\psi$, and a is the effective phase modulation amplitude [4] given by

$$a = \frac{4q}{\nu_m}. \tag{22}$$

Since the greatest effect on particle motion would occur at a resonance condition, when the modulation tune was near the island tune, the effective phase modulation amplitude a would be greatly enhanced at a smaller island

tune. The numerical simulations with $q = 0.002$ reported in Ref. [7] and the experiment with $q = 2.04 \times 10^{-4}$ reported in Ref. [9] corresponded to an effective phase modulation amplitude of $a \approx 0.16$. The effective phase modulation amplitude in our system is enhanced by a factor of about 20 in comparison with that of Ref. [7], where the island tune used in numerical simulations is about 0.05. This means that our system is much more sensitive to the tune modulation than that of Ref. [7].

Using parameters obtained from the preceding section for the Hamiltonian, we found that $\nu_{\text{island}} = 4\sqrt{2Eg}$ varied between 0.0026 and 0.0021 depending on the energies of the corresponding tori in the resonance island width. For a given torus at the maximum phase amplitude $\hat{\psi}_4$, the actual island tune $\tilde{\nu}_{\text{island}}$ is given by

$$\tilde{\nu}_{\text{island}} = \frac{\pi \nu_{\text{island}}}{2K(\sin^2 \frac{\hat{\psi}_4}{2})},$$

where K is the complete elliptical integral of the first kind. Since the ν_{island} does not vary appreciably within the island width, Eq. (21) is equivalent to the parametric resonance equation with phase modulation [3,4].

When the modulation frequency is far away from the resonant frequency, the solution of the forced pendulum equation of Eq. (21) is given by a linear superposition of the particular and the general solutions resulting in a beat tune of $|\nu_m - \tilde{\nu}_{\text{island}}|$. The phase oscillation of ψ_4, shown in the middle of Fig. 1(b), exhibited this beating feature for about 900 orbital revolutions, or 225 island turns. The reason that the beating of the phase oscillation in the transverse resonance motion with tune modulation does not persist for a long time is due to a very large equivalent phase modulation amplitude. The resulting response amplitude becomes too large to be confined inside the resonance island.

At the modulation amplitude of $q = 0.000\,86$, the corresponding phase modulation amplitude is $a \approx 1.3$. Numerical simulations of single particle synchrotron motion with rf phase modulation indicated that particles could be driven out of the rf bucket at a modulation amplitude of $a \approx 0.1$ if the separatrix of the modulation Hamiltonian passed through the initial phase space coordinates of the trapped particles [4]. This means that particles can be driven out of the resonance island if the modulation frequency is exactly at the bifurcation frequency with a modulation amplitude greater than $6. \times 10^{-5}$. A word of caution is that only coherent motion of the beam can be measured, i.e., the measured data correspond to the centroid of the beam charge distribution, therefore the measured tolerable modulation amplitude may be different from that predicted by the single particle dynamics.

To characterize the response of a strong phase modulation, we define the critical number of revolutions N_c as the number of revolutions required for the bunch to escape the island. Figure 3 shows $\frac{1}{N_c}$ vs the modulation frequency $f_m = \nu_m f_0$ with $q = 0.000\,86$. The error bar reflects both the uncertainty in determining the number of revolutions that the particle stays inside the island and the range of variations in N_c for different experimental

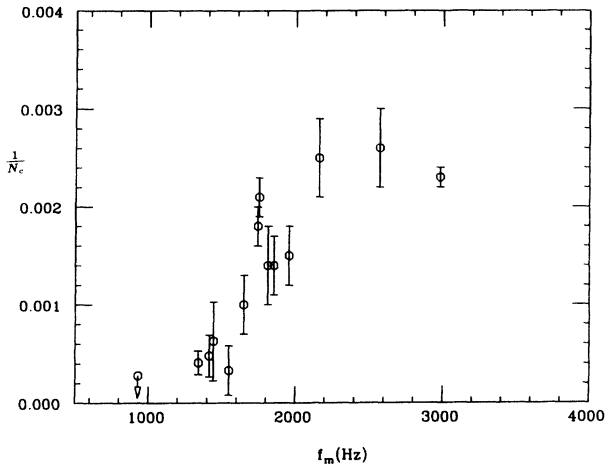

FIG. 3. The response $\frac{1}{N_c}$, where N_c is the number of orbital revolutions that the particle stays inside resonance islands, is plotted as a function of the modulation frequency at the modulation amplitude of $q = 0.000\,86$. Note here that the error bar is much larger in the transition frequency region, where N_c varied wildly in different runs. This reflected the fact that N_c depended sensitively on the initial condition. The error bars are too large to identify subharmonic excitations.

runs. A larger error bar could indicate that the result depended very much on the initial beam conditions. At low modulation frequencies, an apparent increase in response seems to occur for $f_m \geq f_c = 1200 \pm 200$ Hz. At the high modulation frequency end, the response continues to be large up to our system limitation of 3 kHz. Thus the response function has the characteristic of the parametric resonance system [3,4]. Unfortunately, our modulation system was limited to 3 kHz due to the vacuum chamber thickness and the limitation of our modulation power supply.

Figure 4 shows $\frac{1}{N_c}$ as a function of the modulation amplitude q at the modulation frequency of $f_m = 1545$ Hz. Here a strong response seems to occur at $q \geq q_c =$

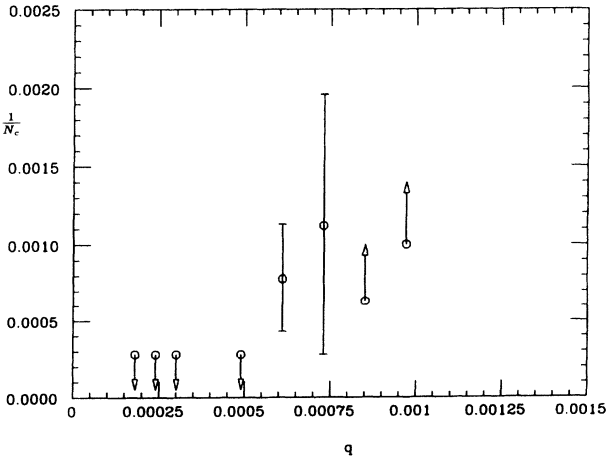

FIG. 4. The response $\frac{1}{N_c}$ is plotted as a function of the modulation strength q for the modulation frequency of 1545 Hz. It appears that there is a sudden onset of strong response to the island motion at the modulation amplitude of $q_c \approx 0.0006$.

0.0006 ± 0.0001, where q_c denotes the critical modulation amplitude. Since the modulation frequency of 1545 Hz is much smaller than the island frequencies of 2160–2720 Hz, depending on the energy of the torus, the response can be expressed as a *linear superposition* of the particular and the general solutions of the linearized Eq. (21). Assuming that the initial phase space coordinates of the trapped bunch were located close to the center of the island, the maximum response becomes

$$\hat{\psi}_4 \approx \frac{2 \times 4\nu_m q}{\tilde{\nu}^2_{\text{island}}(\hat{\psi}_4) - \nu_m^2}, \tag{23}$$

where the factor of 2 arose from the linear superposition of two solutions (see, e.g., [3]). At the modulation amplitude of $q = 0.0006$, the maximum phase amplitude $\hat{\psi}_4$ can become large and therefore particles can be driven out of resonance islands.

C. Comparison with theoretical models

Following Ref. [6], a dynamical system becomes chaos when both of the following conditions:

$$\eta \geq \frac{|1 - \xi^2|}{\xi}, \tag{24}$$

$$\eta \leq \frac{64}{\pi \xi^3}, \tag{25}$$

are satisfied, where the dimensionless parameters, ξ and η, are given by

$$\xi = \frac{\nu_m}{\nu_{\text{island}}}, \quad \eta = \frac{mq}{\nu_{\text{island}}}.$$

The parameter η is equivalent to the phase modulation amplitude a of Eq. (22) at $\nu_m \approx \nu_{\text{island}}$. The condition for chaos given by Eq. (24) is identical to Eq. (23) with an amplitude independent island tune and a maximum phase amplitude of $\hat{\psi} = 2$ rad. The condition of Eq. (25) corresponds to the overlapping of modulation sidebands. On the other hand, Ref. [7] obtained the threshold for the chaotic transition by imposing the stability condition to the phase space maps along the separatrix trajectory. The critical modulation amplitude is given by

$$\eta \geq \frac{2w_{\text{SL}}}{\pi \xi^2} \cosh \frac{\pi \xi}{2}. \tag{26}$$

Here w_{SL} signifies the critical width of the stochastic layer [7], which is given by the relative energy deviation from the separatrix torus.

Figure 5 shows curves for the critical η as a function of ξ. The curve for Eq. (24) is marked with (a), the curve for Eq. (26) is marked with (b1), (b3), and (b5) for the stochastic layer width parameter $w_{\text{SL}} = 0.1$, 0.3, and 0.5 respectively, and the curve for Eq. (25) is marked with (c). The experimental data points shown with square symbols correspond to the critical frequency and strength obtained from Figs. 3 and 4, i.e., $q = 0.000\,86$, $f_m = 1200$ Hz and $q = 0.0006$, $f_m = 1545$ Hz. The data, shown as circles in Fig. 5, were taken from Ref. [9], where the

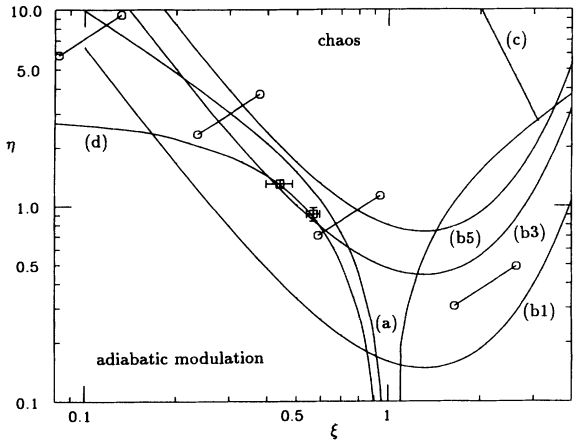

FIG. 5. The chaotic transition conditions are shown as curve (a) for Eq. (24), as curves (b1), (b3), and (b5) for $w_{\text{SL}} = 0.1$, 0.3, and 0.5, respectively, for Eq. (26), and as curve (c) for Eq. (25). The horizontal axis in this figure is $\xi = \frac{\nu_m}{\nu_{\text{island}}}$ and the vertical axis is $\eta = \frac{mq}{\nu_{\text{island}}}$. The square symbols correspond to the data of transition point of Figs. 3 and 4, where the island tune is taken as $\nu_{\text{island}} = 0.002\,63$. The data shown as circles were taken from Ref. [9] with quoted island tune range from 0.0053 to 0.0085.

range of the quoted island tune, from 0.0053 to 0.0085, was assumed. The uncertainty (error bar) of these data points is relatively large due to the uncertainty in the island tune, which has not been measured directly in the experiments of Ref. [9].

Note here that ξ, η parameters of this experiment (square symbols) are lying on a curve with a stochastic width of $w_{\text{SL}} = 0.3$. It is possible although fortuitous to relate the critical stochastic width of $w_{\text{SL}} = 0.3$ to the energy difference between the tori of the SFP and the UFP, i.e.,

$$\frac{E_{\text{SFP}} - E_{\text{UFP}}}{E_{\text{SFP}}} = \frac{4|g|}{|\alpha| + 2|g|} \approx 0.3. \tag{27}$$

For a parametric resonant system with phase modulation [Eq. (21)], the amplitude response increases dramatically when the bifurcation frequency of the system is encountered [3,4]. The bifurcation frequency corresponds to the onset of generating a pair of SFP and UFP beside the original SFP within the original island of the nonlinear resonance. For each additional SFP, there is an associated *secondary* island. If the modulation amplitude q is increased at a constant modulation frequency below the bifurcation frequency, the size of the outer secondary island increases accordingly. Therefore particles in the nonlinear resonance island will be driven out of the inner secondary island and will travel along the separatrix of the nonlinear resonance. Similarly, when the modulation frequency increases toward the bifurcation frequency, at a constant modulation amplitude η, the secondary separatrix created by the tune modulation will cut through the center of the unperturbed nonlinear resonance island. Thus it is useful to characterize the transition to a large response function by the onset of the bifurcation transi-

tion in the parametric resonant system. The bifurcation tune parameter ξ_b is related to the modulation amplitude parameter η by [2–4]

$$\xi_b = 1 - \frac{3}{16}(4\eta)^{2/3}, \tag{28}$$

which is shown as the curve marked (d) in Fig. 5. Note that Eq. (28) is valid only near and below the island frequency. Equation (28) seems to imply that the tolerable modulation amplitude is zero at $\xi = 1$. This is, however, not the case due to the nonlinearity of the system in Eq. (21). At the bifurcation frequency, the stable fixed point amplitude is $\hat{\psi}_{4,\mathrm{SFP}} = 2(4\eta)^{1/3}$ and the amplitude of the SFP at $\xi = 1$ becomes $(8\eta)^{1/3}$. Therefore there is a minimum modulation strength η_c given by

$$\eta_c \geq \frac{c}{8} \quad (c \approx 1),$$

so that the resulting response amplitude is large, i.e., $\hat{\psi}_4 \approx c^{1/3}$. In the region $\xi > 1$, i.e., the modulation frequency is higher than the island frequency, there is only one SFP within each nonlinear resonance island. The critical tune modulation amplitude may be given by either Eq. (23) or Eq. (26). More measurements of the critical modulation amplitude as a function of modulation frequency are necessary to compare to these theoretical models.

IV. CONCLUSION

Effects of the tune modulation on the motion of particles trapped in resonance islands were studied experimentally. The beam was observed for the first time traveling from near the center of resonance islands toward the separatrix of the Hamiltonian due to the betatron tune modulation. We characterized the response of the trapped particle by $\frac{1}{N_c}$, where N_c is the number of orbital revolutions that the beam remains trapped inside a resonance island. The dynamics is similar to that of the synchrotron motion with an equivalent phase modulation. The response, when plotted as a function of modulation frequencies, displayed characteristics of a parametric resonant system [3,4]. The measured response, when plotted as a function of the modulation amplitude, exhibited the existence of a critical modulation amplitude, where particles can easily be driven out of the resonance islands. These critical modulation amplitudes and frequencies are compared with chaotic transition conditions of Refs. [6,7] and the bifurcation condition of Ref. [4]. Further experiments with a detailed exploration of phase space maps as a function of modulation frequency at a smaller modulation amplitude, e.g., an equivalent phase modulation amplitude of $a < 0.5$, and at higher modulation frequencies, where theoretical models differ greatly, would be valuable.

It is generally known that the stochasticity begins at a region of phase space around unstable fixed points. However, the particle beam cannot easily be tracked experimentally along the separatrix due to the fact that particles in the beam bunch can split into small groups leading to a strong decoherence for the centroid of the charge distribution. However, careful experimental observations of Poincaré maps inside the island may lead to further insight for theoretical studies. Since the equation of the phase oscillation, in the presence of betatron tune modulation, differs in details from that of the driven pendulum equation, more rigorous theoretical treatment is needed. Numerical simulations in many realistic dynamical systems are also needed. These studies can help to gain theoretical insight for rigorous treatment of dynamical systems.

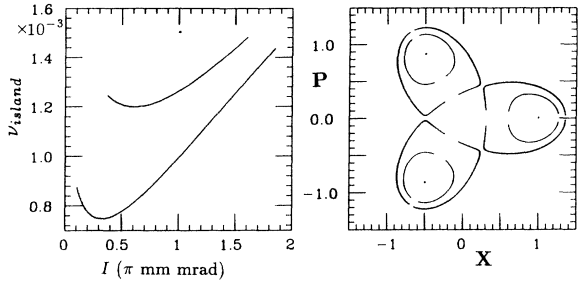

FIG. 6. The Poincaré maps of three tori in third-order resonance islands are plotted in the right figure and the corresponding square root of spring constant "ν_{island}," for the betatron phase oscillation as a function of the action of each torus, are plotted in the left figure. The phase space coordinates are $X = \sqrt{I}\cos\psi$ and $P = -\sqrt{I}\sin\psi$. The parameters of the resonance Hamiltonian are $\delta = 1/2000$, $\alpha = -1/1000$ $(\pi\,\mathrm{mm\,mrad})^{-1}$, and $g = 1/3000$ $(\pi\,\mathrm{mm\,mrad})^{-1/2}$.

ACKNOWLEDGMENTS

We thank Dr. Frank Zimmermann for his useful comments. This work is supported in part by grants from the National Science Foundation, Grant No. NSF PHY-9221402, and from the U.S. DOE, Grant No. DE-FG02-93ER40801.

APPENDIX: AN EXAMPLE FOR THE THIRD-ORDER RESONANCE

We consider an illustrative example for the third-order resonance with parameters $\delta = 1/2000$, $\alpha = -1/1000$ $(\pi\,\mathrm{mm\,mrad})^{-1}$ and $g = 1/3000$ $(\pi\,\mathrm{mm\,mrad})^{-1/2}$. The corresponding SFP and UFP are located at $I_{\mathrm{SFP}} = 1$ $(\pi\,\mathrm{mm\,mrad})$, $I_{\mathrm{UFP}} = 0.25$ $(\pi\,\mathrm{mm\,mrad})$. Three tori and their corresponding "island tune" $\nu_{\mathrm{island}} = \sqrt{G}$, for the phase oscillations of ψ_3 are shown, respectively, in the right and the left frames of Fig. 6. Note here that the spring constant for the phase oscillation varies by about a factor of 4 for a torus near the separatrix. The island tune at the SFP is 0.0015.

[1] B.V. Chirikov, Phys. Rep. **52**, 263 (1979).
[2] M. Syphers *et al.*, Phys. Rev. Lett. **71**, 719 (1993); Y. Wang *et al.*, Phys. Rev. E **49**, 1610 (1994).
[3] M. Ellison *et al.*, Phys. Rev. Lett. **70**, 591 (1993).
[4] H. Huang *et al.*, Phys. Rev. E **48**, 4678 (1993).
[5] D. Li *et al.*, Phys. Rev. E **48**, 1638 (1993).
[6] T. Chen and S. Peggs, in *Proceedings of the 3rd ICFA Beam Dynamics Workshop, Novosibirsk*, edited by I. Koop and G. Tumaikin (INP, Novosibirsk, 1989), p. 98.
[7] F. Zimmermann, in *Stability of Particle Motion in Storage Rings*, edited by M. Month, A.G. Ruggiero, and W.T. Weng, AIP Conf. Proc. No. 292 (AIP, New York, 1992), p. 273.
[8] X. Altuna *et al.*, in *Advanced Beam Dynamics Workshop on Effects of Errors in Accelerators, Their Diagnosis and Correction*, AIP Conf. Proc. No. 255 (AIP, New York, 1992), p. 355; L. Evans *et al.*, in *Proceedings of the 1st European Particle Accelerator Conference, Rome, 1988*, edited by S. Tazzari and K. Huebner (World Scientific, Singapore, 1989), p. 619; J. Gareyte *et al.*, in *Proceedings of the 1989 IEEE Particle Accelerator Conference, Chicago* (IEEE, New York, 1989), p. 1376; D. Brandt *et al.*, in *Proceedings of the 2nd European Particle Accelerator Conference, Nice* (Editions Frontieres, Gif-sur-Yvette, 1990), p. 1438.
[9] T. Satogata *et al.*, Phys. Rev. Lett. **68**, 1838 (1991); N. Merminga *et al.*, in *Proceedings of the 1989 IEEE Particle Accelerator Conferences, Chicago*, Ref. [8], p. 1429.
[10] G. Guignard, CERN Report No. 76-06, 1976 (unpublished).
[11] S.Y. Lee *et al.*, Phys. Rev. Lett. **67**, 3768 (1991); D.D. Caussyn *et al.*, Phys. Rev. A **46**, 7942 (1992).
[12] M. Ellison *et al.*, in *Stability of Particle Motion in Storage Rings* (Ref. [7]), p. 170.
[13] This experiment was performed in January, 1992, when our hardware was capable only of digitizing two positions with 4096 data points, which include 512 data points prior to the kick. At present, our improved hardware is capable of detecting 6D phase space with 256 000 data points.
[14] J.Y. Liu *et al.*, Phys. Rev. E **49**, 2347 (1994).
[15] J. Budnick and G.D. Randeau, in *Proceedings of the IEEE Nuclear Science Symposium and Medical Imaging Conference, Orlando, FL*, edited by G. T. Alley (IEEE, New York, 1992), p. 566.